THE JOURNAL OF BIOLOGICAL CHEMISTRY VOL. 287, NO. 46, pp. 39205–39215, November 9, 2012

The Importance of TM3-4 Loop Subdomains for Functional Reconstitution of Glycine Receptors by Independent Domains*

Received for publication, April 26, 2012, and in revised form, September 17, 2012 Published, JBC Papers in Press, September 20, 2012, DOI 10.1074/jbc.M112.376053

Bea Unterer[1], **Cord-Michael Becker, and Carmen Villmann**[2]

From the Institute of Biochemistry, Emil Fischer Center, Friedrich-Alexander University Erlangen-Nuernberg, Fahrstrasse 17, 91054 Erlangen, Germany

Background: Truncated non-functional GlyRs are reconstituted in channel function by co-expression with a C-terminal domain.
Results: TM3-4 loop residues are expressed independently of TM4 and the truncated GlyR.
Conclusion: TM4 and the C terminus are not sufficient to rescue GlyR function; rather, residues of the TM3-4 loop are required.
Significance: TM3-4 loop residues trigger directly or indirectly conformational changes necessary for GlyR functionality.

Truncated glycine receptors that have been found in human patients suffering from the neuromotor disorder hyperekplexia or in spontaneous mouse models resulted in non-functional ion channels. Rescue of function experiments with the lacking protein portion expressed as a separate independent domain demonstrated restoration of glycine receptor functionality *in vitro*. This construct harbored most of the TM3-4 loop, TM4, and the C terminus and was required for concomitant transport of the truncated α1 and the complementation domain from the endoplasmic reticulum toward the cell surface, thereby enabling complex formation of functional glycine receptors. Here, the complementation domain was stepwise truncated from its N terminus in the TM3-4 loop. Truncation of more than 49 amino acids led again to loss of functionality in the receptor complex expressed from two independent domain constructs. We identified residues 357–418 in the intracellular TM3-4 loop as being required for reconstitution of functional glycine-gated channels. All complementation constructs showed cell surface protein expression and correct orientation according to glycine receptor topology. Moreover, we demonstrated that the truncations did not result in a decreased protein-protein interaction between both glycine receptor domains. Rather, deletions of more than 49 amino acids abolished conformational changes necessary for ion channel opening. When the TM3-4 loop subdomain harboring residues 357–418 was expressed as a third independent construct together with the truncated N-terminal and C-terminal glycine receptor domains, functionality of the glycine receptor was again restored. Thus, residues 357–418 represent an important determinant in the process of conformational rearrangements following ligand binding resulting in channel opening.

Glycine is the major inhibitory neurotransmitter in the brainstem and spinal cord in humans and rodents. Following binding to its postsynaptic receptor, an intrinsic chloride channel will be opened. The glycine receptor (GlyR)[3] undergoes a developmental shift after birth, with a replacement of homomeric α2 receptors representing the embryonic GlyR isoform ($GlyR_N$) by the adult heteromeric α1β or α3β configuration ($GlyR_A$) (1, 2). The adult pentameric receptor complex is composed of two α and three β subunits (2α1/3β or 2α3/3β) (3, 4) and anchored via gephyrin to the cytoskeleton. GlyRs belong to the superfamily of Cys-loop receptors as well as $GABA_{A/C}$ receptors, nicotinic acetylcholine receptors, and the $5HT_3$ receptor. The Cys-loop in the extracellular N terminus of the receptor proteins is conserved among all family members, whereas GlyRs harbor an additional disulfide bond in the extracellular loop C (5). Each subunit exhibits a large extracellular N terminus, four transmembrane domains (TMs) connected by intra- or extracellular loop structures with TM2 facing the ion channel pore, and an extracellular C terminus. The x-ray structure analysis of homologous proteins as the acetylcholine-binding protein and the prokaryotic ligand-gated ion channels ELIC (cloned from *Erwinia chrysanthemi*) and GLIC (from *Gloeobacter violaceus*) provided lots of structural information on the N terminus, the TMs, and the short loops between TM1-2 and TM2-3, except for the large intracellular loop between TM3 and TM4 (6, 7). This intracellular domain (iD) shows the highest variability among all Cys-loop receptors and seems to have developed late in evolution because the prokaryotic isoforms ELIC and GLIC lack this domain. Previous reports have shown that this domain is involved in receptor trafficking and anchoring. Anchoring is facilitated via interaction of the GlyRβ TM3-4 loop with E-domain monomers of gephyrin, which forms a hexagonal lattice structure at the postsynaptic density (8, 9). Two basic motifs near TM3 and TM4 in GlyRα1 were found to interact with Gβγ subunits, which enhances the apparent glycine affinity of the receptor and results in an increase in ion channel

* This work was supported by Deutsche Forschungsgemeinschaft Grant VI586, EU Neurocypres, and the Johannes und Frieda Marohn Stiftung.
[1] Present address: Institute for Clinical Neurobiology, University of Wuerzburg, D-97078 Wuerzburg, Germany.
[2] To whom correspondence should be addressed: Julius-Maximilians-University Wuerzburg, Institute for Clinical Neurobiology, Versbacherstr. 5, D-97078 Wuerzburg, Germany. Tel.: 49-931-201-44035; Fax: 49-931-201-44009; E-mail: Villmann_C@klinik.uni-wuerzburg.de.

[3] The abbreviations used are: GlyR, glycine receptor; TM, transmembrane domain; iD, intracellular domain; trc, truncated; HEK, human embryonic kidney; ER, endoplasmic reticulum.

open probability (10). Recently, pharmacological modulation of the GlyRα1 via the TM3-4 loop has been reported for ethanol as well as propofol (11, 12). In contrast, the TM3-4 loop seems not to be important for signal transduction in general because a replacement of this large domain in $GABA_C$ and the $5HT_3$ receptor by the short linker present in GLIC still resulted in functional ion channels (13). A lack of the TM3-4 loop, TM4, and the C terminus as present in the mouse model *oscillator*, however, results in non-functionality of the GlyR complex. A coexpression of those truncated N-terminal receptor domains (α1-trc) together with the lacking domain as a separate construct resulted in rescue of ion channel functionality, thus demonstrating that GlyRs are composed of independently folding domains (14). Rescue efficiency was largely dependent on the presence of the basic motif RRKRRH in the α1-trc at its C-terminal end. This motif has previously been shown to be important for surface integration and subunit-specific sorting (15, 16).

In the present study, we have investigated protein-protein interactions within GlyRα1 protein when coexpressed from two independently folding domains. Truncated GlyRs result in non-functionality. Coexpression with the lacking protein domain regained functional channels. We truncated the complementation construct harboring parts of the TM3-4 loop, TM4, and the C terminus from its N-terminal end. With a deletion of more than 49 residues, functionality was again almost abolished. Truncation of 62 amino acids never resulted in a functional ion channel configuration. Therefore, residues Ser^{406}–Glu^{411} localized at the interface between the last variable (V2) and constant (C3) region before TM4 (Fig. 1) are critical for ion channel reconstitution from two independent domains. Cell surface expression and correct membrane orientation corresponding to GlyR topology were demonstrated for all GlyR domain constructs. Finally, protein-protein interactions of the N-terminally truncated α1-trc together with the complementation constructs were not disturbed. Moreover, the constituted two-domain receptor seemed to fail at the transduction of ligand binding into channel opening. This disability was conquered by coexpression with the 62 amino acids of TM3-4 loop(357–418) as a third independent construct. Thus, functional GlyRs can be rebuilt from three small independent domains, substantiating the mosaic structure of Cys-loop receptors.

EXPERIMENTAL PROCEDURES

Transfection of HEK293 Cells—HEK293 (human embryonic kidney) cells were grown in Earle's minimal essential medium (PAA Laboratories), supplemented with 10% fetal calf serum, L-glutamine (200 mM), and 50 units/ml penicillin and streptomycin at 37 °C and 5% CO_2. 24 h after splitting (2×10^6 cells for a 10-cm dish; $0{,}15 \times 10^6$ cells for a 3-cm dish), the cells were transiently transfected using the calcium phosphate precipitation method (17). Cell culture medium was replaced 24 h after transfection.

Preparation of Whole-cell Lysates—Whole cell lysates were prepared 48 h post-transfection by adding 500 μl of preheated 2× SDS sample buffer onto a 10-cm dish of transfected HEK293 cells. The samples were heated for 10 min at 95 °C before application to SDS-PAGE.

Membrane Protein Preparation—The preparation was performed 48 h post-transfection with HEK293 cells grown in 10-cm dishes as described above. After detaching the cells with cold 1× PBS (PAA Laboratories) and centrifugation (10 min, 1000 × *g*), the cell pellet was resuspended in 3 ml of buffer H (10 mM potassium phosphate buffer, pH 7.4, 250 mM EDTA, 250 mM EGTA, and protease inhibitor mixture tablets; Roche Applied Science). The probes were homogenized in a tapered glass tissue grinder and with an Ultra-Turrax disperser, followed by centrifugation for 10 min at 16,000 × *g*. Afterward, the pellets were resolved in buffer H, and the homogenization and centrifugation step was repeated once. The pellets were resolved in buffer B (25 mM potassium phosphate buffer, pH 7.4, 200 mM KCl, 250 mM EDTA, 250 mM EGTA, and protease inhibitor mixture tablets; Roche Applied Science).

Biotinylation of Cell Surface Proteins—The biotinylation assay was performed 48 h post-transfection with HEK293 cells grown in 10-cm dishes as described above. After removing the cell culture medium and three washing steps with cold 1× PBS (PAA Laboratories), the surface proteins were labeled with EZ-Link Sulfo-NHS-LC-Biotin (sulfosuccinimidyl-6-(biotin-amido)-hexanoate (Pierce) for 30 min, followed by washing with quenching buffer (192 mM glycine, 25 mM Tris in PBS, pH 8.0) for 10 min. The cells were detached with ice-cold 1× PBS and centrifuged for 10 min at 1000 × *g*, followed by cell lysis with TBS (Tris-buffered saline with 1% Triton X-100 and protease inhibitor mixture tablet; Roche Applied Science) and a 1-min centrifugation step at 13,000 × *g*. The supernatant (whole protein fraction) was incubated with 50 μl of streptavidin-agarose beads (Pierce) for 2 h at 4 °C while rotating. After removing the supernatant and washing the beads three times in TBS, the biotinylated proteins were eluted by boiling with 50 μl of 2× SDS sample buffer for 5 min.

Co-immunoprecipitation—Transfected HEK293 cells were grown on 10-cm dishes as described above and used 48 h after transfection. After washing the cells on ice with cold 1× PBS three times, 600 μl of lysis buffer (20 mM Tris-HCl, 160 mM NaCl, 5 mM EDTA, 1 mM DTT, 1% Triton X-100, protease inhibitor mixture tablets, pH 7.4) was added at each plate to scrape off the cells. After centrifugation (10 min, 4 °C, and 15,000 rpm) the supernatant (lysate) was used as input for co-immunoprecipitation experiments. To 600 μl of the respective solution, 2 μl of MAb2b antibody (1:200; Synaptic Systems) and 60 μl of protein A-Sepharose beads (1:1 slurry; Sigma) were added and agitated overnight at 4 °C. Then the supernatant was removed, and the beads were washed three times (50 mM Tris-HCl, 160 mM NaCl, 5 mM EDTA, 1% Triton X-100, pH 8.0). Proteins were eluted from the beads by incubating in 30 μl of 2× SDS sample buffer at 95 °C for 7 min.

Western Blot Analysis—For SDS-PAGE, 11% or 15% polyacrylamide gels were used, followed by a Western blot on nitrocellulose membranes. Membranes were blocked for 1 h with TBB (TBS + 5% BSA) and incubated for 1 h or overnight (4 °C) with primary antibodies. The secondary antibody was horseradish peroxidase-coupled (incubation for 1 h) for detection with the ECLplus system (GE Healthcare).

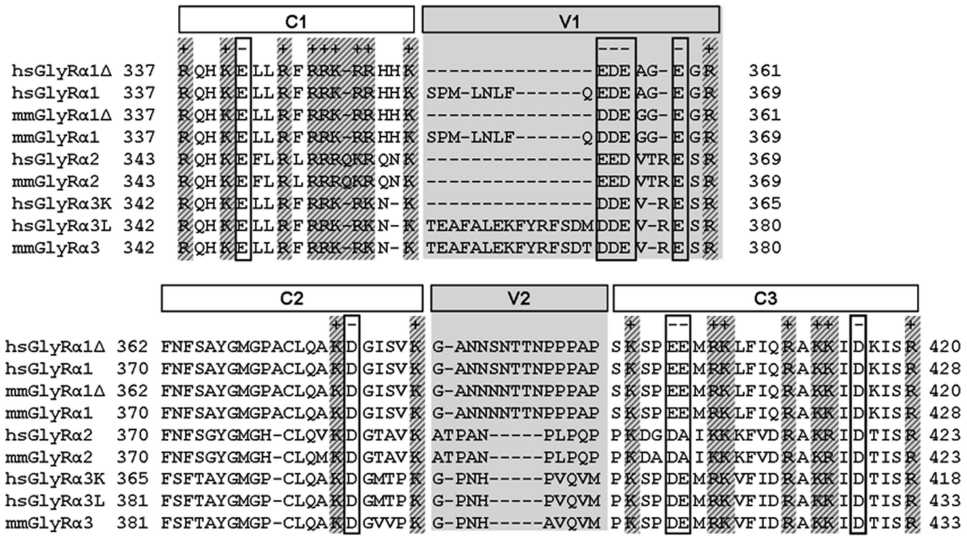

FIGURE 1. **Sequence alignment of various GlyR intracellular TM3-4 loop sequences between amino acids 337 and 433.** The amino acid numbering refers to the immature polypeptide, modified from Melzer *et al.* (15). The length of this loop differs between GlyRα variants due to alternative splicing within the sequence. The sequences of the human (*H. sapiens*; *hs*) and mouse (*M. musculus*; *mm*) TM3-4 loops of the GlyR α1, α2, and α3 subunits (including different splice variants) are shown. The alignment is arbitrarily subdivided into conserved (C1–C3) and variable regions (V1 and V2, *shaded* in *gray*). Most charged amino acids (+, positively; −, negatively) are conserved between all variants.

Immunocytochemistry—Transfected HEK293 cells were grown on polylysine-coated coverslips, fixed with 4% paraformaldehyde and 4% sucrose in PBS (10 min), washed three times with PBS, and blocked as well as permeabilized with 0.1% Triton X-100, 5% donkey serum in PBS (30 min) at room temperature. Cells were incubated with primary antibodies for 1 h at room temperature and washed three times with PBS. This procedure was repeated with secondary antibodies. Finally, cells were embedded in Mowiol and subjected to confocal microscopy on a DMIRE2 confocal microscope (Leica). For live stain, transfected cells were incubated with primary antibody for 1 h at 4 °C before fixation without permeabilization. All experiments were performed 24 h post-transfection.

Antibodies Used—For different stainings, monoclonal mouse anti-GlyRα (1:200; MAb4a, Synaptic Systems; recognized epitope harbors amino acids 96–105 of mature glycine receptor α1 subunit), polyclonal rabbit anti-Myc (1:200, C-19 or A-14, Santa Cruz Biotechnology, Inc.), monoclonal mouse anti-Myc (1:200; 9E10, Santa Cruz) or monoclonal mouse anti-GFP (1:500; Roche Applied Science), rabbit anti-Na^+,K^+ ATPase polyclonal antibody (Chemicon), and polyclonal goat anti-GlyRα1 TM3-4 loop (1:50; H18, Santa Cruz Biotechnology, Inc.) were used as primary antibodies. Secondary antibodies were goat anti-mouse Alexa488 (1:400; Invitrogen), goat anti-rabbit Cy3 and donkey anti-goat Cy5 (both 1:250; Dianova). For live stain, monoclonal mouse anti-GlyRα1 (1:100; MAb2b, Synaptic Systems; antibody raised against amino acids 1–10 of the mature glycine receptor α1 subunit) and polyclonal rabbit anti-Myc (1:50; Santa Cruz Biotechnology, Inc.) were used as primary antibodies. For detection with enhanced chemiluminescence, a goat anti-mouse HRP (1:10,000; Dianova) antibody was utilized as secondary antibody.

Alignment—For multiple-sequence alignments, the sequences and boundaries of the TM3-4 loops were taken from the Uniprot database annotation (18). GlyR subunit variants of the TM3-4 loops from either human (*Homo sapiens*, *hs*), or mouse (*Mus musculus*, *mm*) were subjected to a multiple-sequence alignment using the T-Coffee algorithm (19).

Electrophysiological Recordings—Maximal current amplitudes (I_{max}) were measured by the patch clamp technique in a whole-cell configuration mode. Current signals were amplified with an EPC-9 amplifier (HEKA). 24 h after transfection, whole-cell recordings from HEK293 cells were performed by application of ligand (glycine, 1 mM) using a U-tube system. The extracellular buffer consisted of 137 mM NaCl, 5.4 mM KCl, 1.8 mM $CaCl_2$, 1 mM $MgCl_2$, 5 mM HEPES, pH adjusted to 7.2 with NaOH. The internal buffer was 120 mM CsCl, 20 mM $N(Et)_4Cl$, 1 mM $CaCl_2$, 2 mM $MgCl_2$, 11 mM EGTA, 10 mM HEPES, pH adjusted to 7.2 with CsOH. Recording pipettes were fabricated from borosilicate capillaries with an open resistance of about 4 megaohms. Current responses were measured at a holding potential of −60 mV. All experiments were carried out at room temperatures. *Bar diagrams* show the average value $\bar{\chi}$ of n measurements, and the *error bars* are the S.E.

RESULTS

Generation of Successive N-terminal Truncations of Myc-iD-TM4 of the GlyR—Truncated variants of the GlyR α1 subunit, which have been identified in a family with hyperekplexia (20) and are present in the mouse model *oscillator* (21), lacking most of the intracellular TM3-4 loop, the TM4, and the C terminus (α1-trc representing residues 1–357), are not able to gate Cl^- currents. Coexpressions with a corresponding complementation construct iD-TM4, led to reconstitution of functional ion channels (14). The TM3-4 loop determines the largest part of the complementation construct but also exhibits the highest variability among glycine receptor subunits (Fig. 1) (15). In this study, we aimed at mapping the interaction site between GlyRα1-trc and the C-terminal complementation construct, Myc-iD-TM4 (Fig. 2*A*). The iD of the GlyR can be subdivided into constant (C1–3) regions, which are highly conserved among species, and variable (V1-2) regions (Fig. 1). We gener-

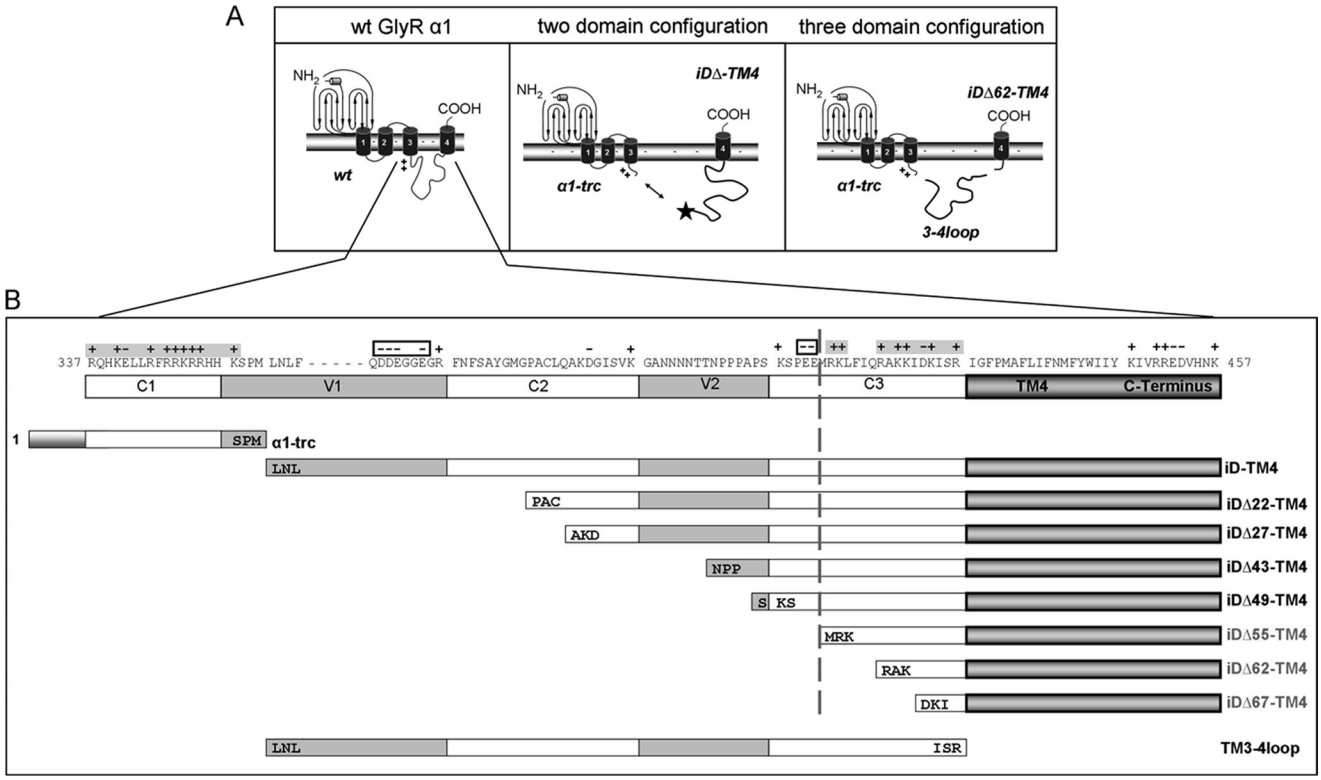

FIGURE 2. **Glycine receptor α1 complementation constructs.** *A*, schematic representation of a single GlyRα1 wild type (*wt*) subunit (*left*) the two-domain configuration (*middle*), and the functional three-domain complementation (*right*). The localization of the Myc epitope for detection of the construct is marked by a *star* (*middle*). Each GlyR subunit consists of a long extracellular N terminus, four transmembrane domains connected by intracellular (TM1-2 and TM3-4) or extracellular (TM2-3) loop structures, and a short extracellular C terminus. The sequence of the long intracellular TM3-4 loop begins with a basic motif, RRKRR, marked by ++. *Middle panel*, the α1-trc domain includes an artificial stop codon at position 356 (which ends with residues SPM; see *B*). The iD-TM4 domain consists of the remaining part of the cytoplasmic TM3-4 loop, the TM4, and the C terminus. The *right panel* shows the three-domain configuration with α1-trc, a truncated complementation construct lacking 62 residues at its N terminus iDΔ62-TM4, and the TM3-4 loop (TM3-4 loop(357–418), representing the lacking 62 residues). *B*, truncated variants, Myc-iDΔx-TM4, lack amino acids at the construct's N terminus. The numbering is relative to the first amino acid of the immature polypeptide. The TM3-4 loop was subdivided into constant (*C1–C3*) and variable (V1 and V2) regions. Positive (+) as well as negative (−) residue charge is indicated *above* the sequence. The α1-trc and all complementation constructs are depicted by *bars* according to their size, with the first three amino acids of the appropriate construct included (*e.g.* iD22-TM4 starts with the amino acid residues PAC at the N-terminal end). The TM3-4 loop (TM3-4 loop(357–418)) begins with ^{357}LNL and ends with residues ISR^{418}).

ated successive N-terminal truncations of the complementation construct (Fig. 2*B*), leading to constructs Myc-iDΔ22-TM4 (lack of V1, subdivision of C2), Myc-iDΔ27-TM4 (subdivision of C2), Myc-iDΔ43-TM4 (subdivision of V2), Myc-iDΔ49-TM4 (division between V2 and C3), Myc-iDΔ55-TM4 (split C3), Myc-iDΔ62-TM4 (lack of V1 to half of C3), and Myc-iDΔ67-TM4 (lack of V1 to almost all of C3), with Δx representing the number of deleted amino acids. For GlyR reconstitution from three independent domains, α1-trc, iDΔ62-TM4, and the TM3-4 loop were coexpressed (Fig. 2*A*, *right*). The construct 3–4 loop harbors amino acid residues 357–418 (TM3-4 loop(357–418) refers to TM3-4 loop further on) (Fig. 2*B*, *bottom*). An N-terminal Myc epitope (9E10) was added for easy immunodetection to either constructs iDΔx-TM4 or the TM3-4 loop (Myc-TM3-4 loop).

Protein Expression of Complementation Constructs—The expression of the generated constructs (Myc-iDΔx-TM4) together with α1-trc was confirmed using crude membrane protein preparations of transfected HEK293 cells. The α1-trc was detected using MAb4a, a monoclonal antibody recognizing an N-terminal epitope of the GlyRα polypeptides. Expression of the complementation constructs was verified with an α-Myc antibody. No significant differences in membrane expression were observed between Myc-iDΔx-TM4 constructs and α1-trc (Fig. 3*A*). A slight decrease for Myc-iDΔ62-TM4 and Myc-iDΔ67-TM4 was determined concomitantly with less coexpressed α1-trc but similar Na^+,K^+ ATPase expression compared with other preparations (*e.g.* with Myc-iDΔ27-TM4). The expression of the Na^+,K^+ ATPase is much higher in untransfected cells; thus, the overexpression of other membrane proteins following transfection seems to reduce the endogenous expression of the Na^+,K^+-ATPase. The surface expression was tested with biotinylation assays of cotransfected HEK293 cells (Fig. 3*B*). In addition to a signal in the whole cell pool and the intracellular/unbound protein fraction, all complementation constructs (iDΔx-TM4, with x representing the number of amino acids deleted, Δ22–Δ67) showed a strong signal at the outer surface of transfected HEK293 cells when coexpressed with α1-trc. Note that complementation constructs harboring TM4 expressed in the absence of α1-trc get transported toward the cell surface only to some extent (14).

Formation of Functional Chloride Channels—The assembly of functional GlyR complexes was analyzed using electrophysiological recordings in a whole-cell configuration of transfected HEK293 cells. The different complementation constructs with N-terminal truncations of up to 67 amino acids were not able to

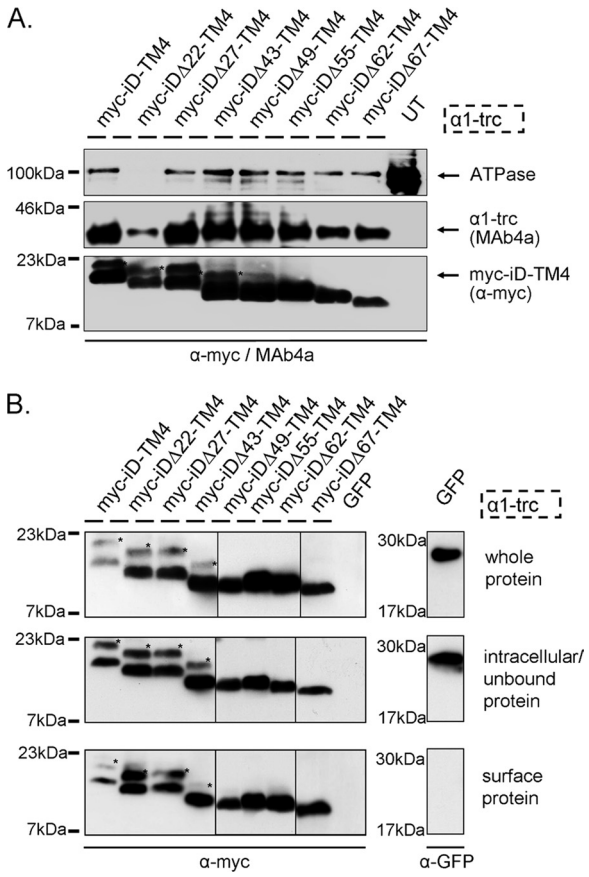

FIGURE 3. **Protein expression of GlyR domains.** *A*, membrane protein expression is shown for α1-trc and the Myc-iDΔ*x*-TM4 constructs. α1-trc exhibits an apparent molecular mass of 37 kDa and was stained with the pan-α antibody MAb4a, recognizing an epitope in the N-terminal portion of all GlyRα proteins. Myc-iDΔ*x*-TM4 constructs (Δ22, Δ27, Δ43, Δ47, Δ55, Δ62, and Δ67) were detected with the α-Myc antibody binding to the 9E10 epitope at their N-terminal ends (see location in Fig. 2*B*). Na^+,K^+-ATPase (*ATPase*) was used as a loading control for membrane proteins (100 kDa) as well as untransfected cells (*UT*) as negative control. Note that the Na^+,K^+-ATPase band was not present in membrane preparations from α1-trc + Myc-iDΔ22-TM4. This does not inevitably mean that Myc-iDΔ22-TM4 was less expressed. Here only half of the protein amount was loaded. The expression of Myc-iDΔ22-TM4 was indistinguishable from other Myc-iDΔ*x*-TM4 constructs in whole cell protein amount, intracellular protein, and cell surface protein; see *B*. *B*, biotinylated protein distribution within transfected HEK293 cells expressing α1-trc in combination with the indicated complementation construct. The *upper blots* depict the Myc-iDΔ*x*-TM4 variants (same constructs used as in *A*) in the whole-cell protein fraction. The *middle panels* illustrate intracellular Myc-iDΔ*x*-TM4, due to continuous overexpression in transfected HEK293 cells and a determined binding capacity of the streptavidin beads used. Myc-iDΔ*x*-TM4 proteins, which are located at the cell surface, were detected with the lower blot (samples were applied onto two gels; *lanes* for Δ49, Δ55, and Δ62 come from a different gel). The negative control for surface expression, GFP, was detectable in the whole-cell protein sample and in the intracellular fraction but not in the surface pool. All blots were stained with either the pan-α GlyR antibody MAb4a or a mouse anti-GFP antibody. *A* and *B*, Myc-iDΔ*x*-TM4 variants differ in their molecular weights according to the amino acids truncated beginning with 20 kDa for Myc-iD-TM4, detected using an α-Myc (9E10) antibody. *, reproducible construct-dependent nonspecific bands using the α-Myc antibody. These bands may result from incomplete signal peptide cleavage.

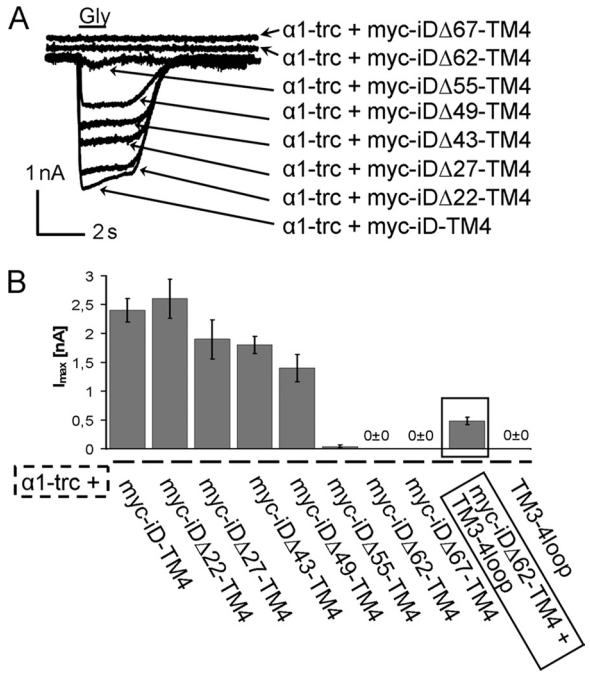

FIGURE 4. **Rescue of function experiments of truncated GlyRα1 variants.** *A*, representative traces of cells transfected with α1-trc and truncated tail variants (Myc-iDΔ*x*-TM4). Maximal glycine-gated currents were determined following 1 mM Gly application in a whole-cell configuration of double-transfected HEK293 cells. Recordings were carried out at −60 mV, $[Cl^-]_{in} = [Cl^-]_{out}$. Agonists were applied via a U-tube for 1 s. The *arrows* point toward the appropriate rescue combinations of α1-trc together with different complementation constructs *B*, bar diagram of the rescue efficiencies determined by the mean I_{max} values with *error bars* representing S.E. The rescue efficiency in a three-domain GlyR configuration is emphasized with a *black frame*. When the TM3-4 loop(357–418) (*3–4loop*) was added as a separate expression construct to a nonfunctional two-domain configuration (α1-trc and Myc-iDΔ62-TM4), receptor function was again restored, although with low efficiency (compare α1-trc + Myc-iDΔ62-TM4 with α1-trc + Myc-iDΔ62-TM4 + TM3-4 loop(357–418)).

gate any Cl^- currents when expressed alone (data not shown). Isolated expression of α1-trc did not lead to functional ion channels either. Coexpression of α1-trc together with Myc-iD-TM4, however, rescued functional Cl^- channels (Fig. 4) (14). The ion channel complementation with Myc-iDΔ22-TM4 rescued the Cl^- influx with efficiency comparable with the full-length Myc-iD-TM4 variant. The rescues with the truncated variants Myc-iDΔ27-TM4, Myc-iDΔ43-TM4, and Myc-iDΔ49-TM4 showed decreased I_{max} values. Maximal currents of α1-trc with Myc-iDΔ27-TM4 reached 79% (1,9 ± 0,34 nA) and with Myc-iDΔ43-TM4 75% (1,8 ± 0,15 nA) of the rescue efficiency compared with the full-length Myc-iD-TM4 variant. The observed GlyR rescue efficiency for Myc-iDΔ49-TM4 was further decreased to 58% (1.4 ± 0.027 nA, Table 1). All glycine-gated currents in a two-domain approach were non-desensitizing, as observed for full-length GlyRα1. Therefore, truncations up to 49 amino acids did not change GlyR channel properties, such as desensitization behavior (Fig. 4*A*). Larger truncations of the complementation construct led to an almost complete loss of rescue efficiency. With the Myc-iDΔ55-TM4 variant, responses were only observed in two of 10 cells recorded. The two most extensive truncations (Myc-iDΔ62-TM4 and Myc-iDΔ67-TM4) led to a complete disappearance of glycine-evoked currents in at least three different batches of cells (Fig. 4*B*). Constructs iDΔ55-TM4, iDΔ62-TM4, and iDΔ67-TM4 generated positively charged N termini with RK at the beginning of iDΔ55-TM4, RAK for iDΔ62-TM4, and KISR for iDΔ67-TM4. This could hinder an interaction with the intracellular C terminus of α1-trc, which is also positively charged. Previously, it was shown that an addition of the positively

TABLE 1

Whole-cell maximal currents [I_{max}] of various coexpressed GlyR domains

HEK293 cells expressing different GlyR variants were patched 24 h post-transfection. Maximal currents (I_{max}) ± S.E. gated with 1 mM glycine were recorded in 9–10 cells out of at least three batches of transfected HEK293 cells.

Expressed domains	No. of cells	I_{max}, 1 mM Gly	Normalized I_{max} (% of α1-trc + iD-TM4)
		nA	%
WT α1	9	6.8 ± 0.31	
α1-trc + Myc-iD-TM4	9	2.4 ± 0.20	100
α1-trc + Myc-iDΔ22-TM4	9	2.6 ± 0.34	108
α1-trc + Myc-iDΔ27-TM4	9	1.9 ± 0.34	79
α1-trc + Myc-iDΔ43-TM4	10	1.8 ± 0.15	75
α1-trc + Myc-iDΔ49-TM4	10	1.4 ± 0.24	58
α1-trc + Myc-iDΔ55-TM4	2/10[a]	0.04 ± 0.027	2
α1-trc + Myc-iDΔ62-TM4	10	0 ± 0	0
α1-trc + Myc-iDΔ67-TM4	10	0 ± 0	0
α1-trc + Myc-iDΔ62-TM4 + 3-4 loop	9	0.48 ± 0.063	20
α1-trc + 3-4 loop	10	0 ± 0	0

[a] Only 2 of 10 cells responded to glycine application; I_{max} value in this case includes also non-responding cells.

charged motif RRKRRH to the N terminus of the full-length iD-TM4 abolished ion channel function when coexpressed with α1-trc harboring the same motif at its C-terminal end (14). When the truncated α1 variant present in the mouse mutant *oscillator* was used, harboring GDIT at its C terminus instead of RRHRRH, functional rescue was still observed. Thus, interactions by charged motifs seem to play a role within the TM3-4 loop of the GlyRα1 to permit conformational changes.

Mapping the Interaction Site—Loss of functionality can result from (i) loss of expression or, if expressed, from (ii) loss of an intracellular interaction between the N-terminal truncated α1 variant and the complementation constructs or from (iii) wrong orientation of the complementation construct within the plasma membrane. Because protein expression (i) as well as cell surface localization has been shown for all complementation constructs and α1-trc (Fig. 3, *A* and *B*), lack of expression can be excluded as a reason for non-functionality of the GlyR channels. To test whether an intracellular protein-protein interaction is required for formation of functional ion channels, we performed co-immunoprecipitation assays. The α1-trc construct was cotransfected with one complementation variant (Myc-iD-TM4, Myc-iDΔ22-TM4, Myc-iDΔ27-TM4, Myc-iDΔ43-TM4, Myc-iDΔ49-TM4, Myc-iDΔ55-TM4, Myc-iDΔ62-TM4, or Myc-iDΔ67-TM4) in HEK293 cells. The input was verified for α1-trc stained with Mab4a and iDΔ*x*-TM4 detected with α-Myc (Fig. 5*A*). Following lysis of transfected HEK293 cells, α1-trc was precipitated using the GlyRα1-specific monoclonal antibody MAb2b. More binding capacity of antibody (lower dilution of antibody, 1:150) resulted in more precipitated iDΔ*x*-TM4 protein (Fig. 5*B*, *bottom left panels*). The co-precipitated Myc-iDΔ*x*-TM4 variants were detected with the α-Myc antibody (9E10). A strong interaction was observed for α1-trc coexpressed with the full-length complementation construct Myc-iD-TM4. In contrast to the observed decrease for I_{max} values, protein-protein interaction was not affected with increasing the truncated portion of the complementation constructs at their N-terminal ends (Fig. 5*B*).

Membrane Orientation of the Myc-iDΔ62-TM4 Domain—To exclude the possibility that non-functionality of α1-trc together with shortened complementation constructs (*e.g.* Myc-iDΔ62-TM4) arose from a wrong orientation of the complementation constructs within the plasma membrane, live cell

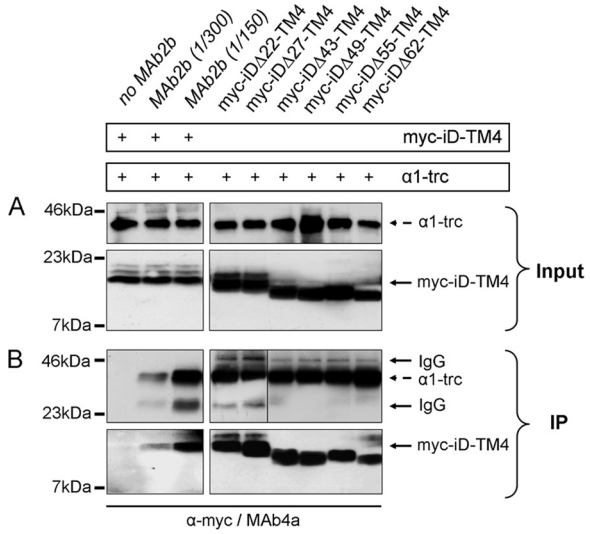

FIGURE 5. **Protein-protein interactions of GlyRα1-trc with various complementation constructs.** *A* and *B*, following cotransfection of α1-trc with one complementation construct, HEK293 cells were lysed (*Input*) and used for immunoprecipitation of α1-trc with the α1-specific GlyR antibody MAb2b binding to a native epitope in the far N-terminal portion of the α1 protein. The complementation constructs, Myc-iDΔ*x*-TM4s, were co-immunoprecipitated (*IP*) and detected with a monoclonal anti-Myc (9E10) antibody. The presence of α1-trc and Myc-iD-TM4 is indicated by a *plus sign*. *A*, the input before co-immunoprecipitation of α1-trc (stained with MAb4a) and the complementation constructs Myc-iDΔ*x*-TM4, with Δ*x* representing Δ22, Δ27, Δ43, Δ49, Δ55, and Δ62. *B*, co-immunoprecipitation (*IP*) in a two-domain receptor configuration. The negative control without any MAb2b showed no unspecific binding (*first lane*, *bottom panel*). Increasing the amount of MAb2b (1:300 or 1:150 dilution) during the immunoprecipitation raised the specific signal for the co-precipitated Myc-iD-TM4. All complementation constructs (Myc-iDΔ*x*-TM4) showed a strong protein-protein interaction with α1-trc. The construct Myc-iDΔ55-TM4 runs reproducibly at a higher apparent molecular weight. The IgG signals (50 and 25 kDa) became visible due to the use of two mouse monoclonal antibodies, one for precipitation (MAb2B) and the other for detection (MAb4a) of the GlyR proteins. *Boxed gel lanes* indicate that samples were run on different gels.

stainings were performed. It has been shown for membrane proteins that there exists a positive inside rule arguing that intracellular domains contain more positively charged amino acid residues than extracellular domains (22, 23). The Myc-iDΔ62-TM4 construct fulfilled the criterion of more positively charged amino acid residues inside than at the extracellular side flanking the transmembrane helix 4. Live staining allows the detection of extracellular epitopes in a native protein configuration before fixation. HEK293 cells cotransfected with α1-trc

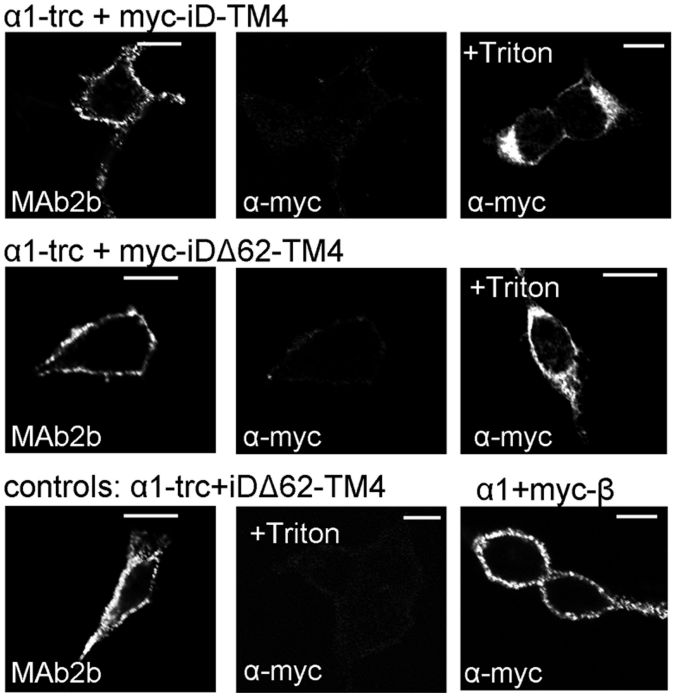

FIGURE 6. **Orientation of Myc-iD-TM4 and Myc-iDΔ62-TM4 within the plasma membrane.** Confocal images of live stained cells are shown. HEK293 cells were transfected with either α1-trc + Myc-iD-TM4 or α1-trc + Myc-iDΔ62-TM4. The α1-trc was detected using MAb2b, and the Myc-iD-TM4 (Myc epitope is fused to the intracellular N terminus) was stained using a α-Myc antibody. As control, fixed and Triton X-100-treated cells showed intracellular protein (*last panels* in the *top* and *middle rows*). As negative control, cells transfected with α1-trc + iDΔ62-TM4 (without any tag) were stained with MAB2a for α1-trc and α-Myc for the iDΔ62-TM4 (last in permeabilized cells, +Triton X-100). Transfected cells with GlyRα1 + GlyRβ + gephyrin were used as positive control for the α-Myc antibody because the GlyRβ was tagged with a Myc epitope at the N-terminal extracellular part. *Scale bars*, 20 μm.

and Myc-iD-TM4 or α1-trc and Myc-iDΔ62-TM4 were used. The extracellular N-terminal GlyRα1 epitope of α1-trc was stained with MAb2b (Fig. 6, *left columns*). Detection of the complementation constructs was performed with an α-Myc antibody (Fig. 6, *middle* and *right columns*). Because the MAb2b epitope is localized extracellularly, the α1 construct served also as a control for transfection. In both coexpressions, Myc staining was observed neither for Myc-iD-TM4 nor for Myc-iDΔ62-TM4 (Fig. 6, *middle panels* in *top* and *middle rows*). Thus, the orientation of both complementation constructs was correct and in agreement with GlyR topology, respectively. These results were corroborated in permeabilized cells, where the Myc epitope localized at the intracellular N terminus of the complementation constructs was recognized (Fig. 6, *right panels* in *top* and *middle rows*). Additionally, cells transfected with α1-trc and a complementation construct without the Myc epitope (iDΔ62-TM4) showed no staining at all, not even in permeabilized cells (Fig. 6, *middle panel* in *bottom row*). As a positive control, N-terminally Myc-tagged GlyRβ coexpressed with gephyrin and GlyRα1 confirmed that the Myc antibody was able to recognize a native Myc epitope (Fig. 6, *right panel* in *bottom row*).

Three-domain Configuration of the Glycine Receptor α1 Subunit—The coexpression of α1-trc with Myc-iDΔ62-TM4 generated no functional ion channels. In contrast, in transfections of α1-trc with full-length Myc-iD-TM4, glycine-induced currents were observed. Non-functionality cannot be due to lack of expression (Fig. 3, *A* and *B*) or a wrong topology of the Myc-iDΔ62-TM4 domain because live cell staining showed correct integration into the plasma membrane (Fig. 6). Since protein-protein interaction was not disturbed (Fig. 5*A*), we wanted to analyze whether a three-domain expression of α1-trc, Myc-iDΔ62-TM4, and the TM3-4 loop domain would overcome the non-functionality of the two-domain configuration. Two additional constructs of the TM3-4 loop were used that start shortly after the basic motif of the cytoplasmic TM3-4 loop and end before TM4, one of them with a Myc epitope (TM3-4 loop and Myc-TM3-4 loop with residues 357–418). To control for expression of these GlyR variants, lysates of transfected HEK293 cells with α1-trc, iDΔ62-TM4 (with Myc epitope), and the TM3-4 loop (with and without Myc epitope) were prepared. After Western blot analysis, the staining with an anti-Myc antibody revealed the expression of the TM3-4 loop constructs (Fig. 7). Next, the intracellular localization of α1-trc, Myc-iDΔ62-TM4, and TM3-4 loop was investigated with immunocytochemical stainings with permeabilization of transfected HEK293 cells (Fig. 7*A*). A pDsRed-ER vector expressing a fusion protein of the ER targeting sequence of calreticulin fused to DsRed or pDsRed-Monomer-Mem encoding GAP-43, a membrane protein, fused to DsRed were co-transfected. All constructs (α1-trc, the TM3-4 loop, and the Myc-iDΔ62-TM4) were detectable in the ER (Fig. 7*A*, *middle panels*). Additionally, all three domains were present at or near the plasma membrane and colocalized with each other and with the membrane marker GAP-43 (Fig. 7*A*, *bottom panels*). Thus, the prerequisites for a functional rescue (expression, co-localization, and membrane localization of all three domains) were fulfilled. The functionality of the three coexpressed domains was investigated using whole-cell recordings of transfected HEK293 cells following glycine application (Fig. 7*C*). No currents were observed with two domains, neither with α1-trc plus the TM3-4 loop nor with α1-trc together with Myc-iDΔ62-TM4 (Fig. 7*C*, *top two traces*). In contrast, the receptor complex formation in a three-domain configuration using α1-trc together with the TM3-4 loop and the Myc-iDΔ62-TM4 was able to gate Cl^- currents (Fig. 7*C*, *bottom trace*). The efficiency of rescue was 20% of the configuration α1-trc with the full-length complementation tail (Figs. 4*B* and 7*C* and Table 1). Accordingly, the 62 amino acids of the TM3-4 loop are required for functionality of the ion channel. In conclusion, all three independent domains were concomitantly targeted to the plasma membrane and formed a functional GlyR configuration.

Protein-Protein Interaction Is Abolished with the Intracellular TM3-4 Loop Peptide—To analyze whether the lacking TM3-4 loop portion is also able to form a protein-protein interaction with α1-trc, we used a three-domain coexpression approach of α1-trc together with Myc-iDΔ62-TM4 and the TM3-4 loop construct (with and without Myc epitope). Both GlyR domains, the TM3-4 loop and the Myc-iDΔ62-TM4, differ only slightly in their molecular weight. Therefore, we coexpressed α1-trc together with the Myc-TM3-4 loop alone to detect a protein-protein interaction between these two constructs. Following input control, α1-trc was precipitated with the antibody MAb2b, and the Myc-TM3-4 loop was detected

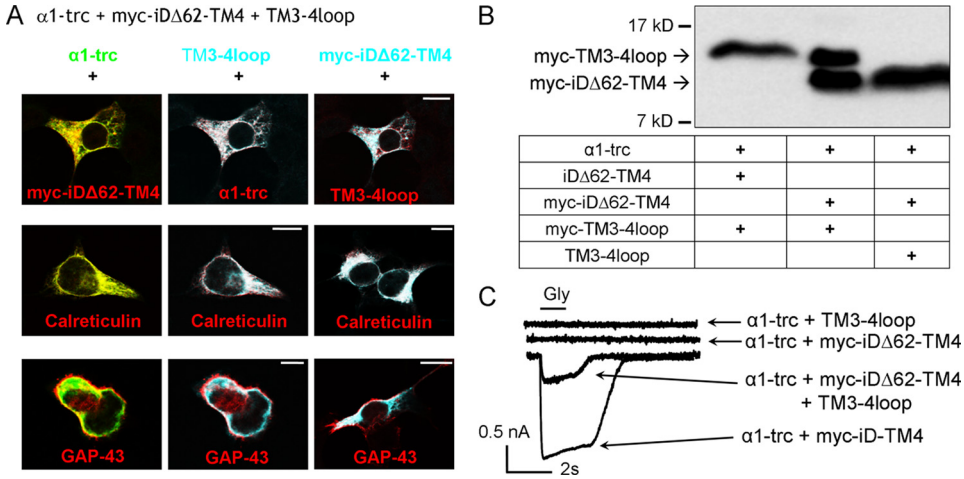

FIGURE 7. **Subcellular localization of independent GlyRα1 domains.** *A*, GlyRα1 domains used in a three-domain GlyR configuration (α1-trc + Myc-iDΔ62-TM4 + TM3-4 loop) were cotransfected into HEK293 cells together with either pDsRed-ER, a vector expressing a fusion protein of the ER targeting sequence of calreticulin fused to DsRed, or pDsRed-Monomer-Mem encoding GAP-43. Overlays of two constructs are shown, with the *color* of each construct indicated by its *letter color*. Cells were fixed and permeabilized prior to staining with MAb4a to recognize the α1-trc variant (shown in *green*) and α-Myc antibody to detect the Myc-iDΔ62-TM4 (depicted in *cyan*) as well as the H18 antibody detecting an epitope within the GlyRα1 TM3-4 loop(357–418) (*cyan*; *TM3-4 loop*). Calreticulin as well as GAP-43 are shown in *red*. The immunoreactivity was visualized by confocal microscopy. *Scale bars*, 20 μm. *B*, whole-cell lysates prepared from HEK293 cells transfected with combinations of α1-trc, (Myc-)iDΔ62-TM4, and (Myc-)TM3-4 loop presence indicated by a *plus sign below* the blot. Both domains, the Myc-TM3-4 loop and Myc-iDΔ62-TM4, were detected via their Myc epitopes. The *arrows* point toward the observed molecular mass of 16 kDa for the TM3-4 loop as well as to 13 kDa for the Myc-iDΔ62-TM4. *C*, functionality of the three-domain receptor configuration. Following glycine application, no functional ion channels were observed using two domains, α1-trc + Myc-iDΔ62-TM4 or α1-trc + TM3-4 loop (*top two traces*). In the three-domain configuration α1-trc + Myc-iDΔ62-TM4 + TM3-4 loop (*middle trace*), however, receptor function was rescued (see *bottom trace* with α1-trc + full-length complementation construct Myc-iD-TM4 for comparison of rescue efficiency). Whole cell recordings of transfected HEK293 cells were used, and maximal Gly-gated currents were determined with 1 mM Gly. Recordings were carried out at −60 mV, $[Cl^-]_{in} = [Cl^-]_{out}$. Agonists were applied via U-tube for 1 s. 9 or 10 cells of each combination were measured in at least three different batches of transfected cells.

with the α-Myc antibody. The construct α1-trc failed to interact with Myc-TM3-4 loop. Next, the α1-trc was coexpressed with the TM3-4 loop (with or without the Myc epitope) together with Myc-iDΔ62-TM4. As shown before, protein-protein interaction was observed for α1-trc and Myc-iDΔ62-TM4 (Fig. 8*B*). The Myc-TM3-4 loop failed again to interact with α1-trc (Fig. 8*B*), although expression of the Myc-TM3-4 loop construct was shown, and this configuration was able to generate functional Cl^- channels (Fig. 8*A*, *bottom panel*). The analysis of the protein-protein interactions between the three GlyR domains demonstrated that α1-trc and Myc-iDΔ62-TM4 have to be inserted in close proximity in the plasma membrane, which in turn allowed interaction and therefore co-precipitation. Instead, the TM3-4 loop construct is a soluble intracellular protein also localized near the surface shown with immunocytochemical stainings. This intracellular peptide may move back and forth, thereby allowing the required movement for channel opening of α1-trc and Myc-iDΔ62-TM4 for at least some channels because the observed rescue efficiency was about 20% of α1-trc plus full-length Myc-iD-TM4. However, we could not exclude the possibility that the intracellular TM3-4 loop domain interacts with other intracellular proteins and/or recruits them to the plasma membrane and that this interaction then triggers conformational changes.

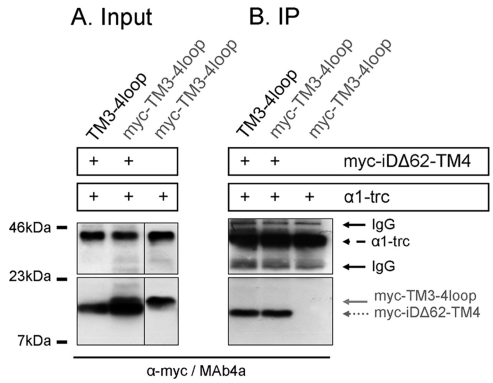

FIGURE 8. **Protein-protein interaction in a three-domain conformation.** The presence of constructs α1-trc and Myc-iDΔ62-TM4 is indicated by a *plus sign*. Furthermore, either the TM3-4 loop construct without an N-terminal Myc epitope or the Myc-TM3-4 loop harboring the Myc epitope was present. *A*, input of α1-trc, Myc-iDΔ62-TM4, and the Myc-TM3-4 loop detected with MAb4a or α-Myc (9E10) antibody. The lower protein band in the input shows Myc-iDΔ62-TM4; the upper band refers to the Myc-TM3-4 loop. Note the small difference in molecular mass between the two polypeptides (Myc-iDΔ62-TM4, 13 kDa; Myc-TM3-4 loop, 16 kDa). *B*, co-immunoprecipitation (*IP*) of the three-domain receptor. Following immunoprecipitation, the TM3-4 loop was never detectable. The *bottom panels* show Myc-iDΔ62-TM4 detected with an α-Myc antibody. The α1-trc was stained concurrently using the pan-α antibody MAb4a.

DISCUSSION

GlyRs are composed of subdomains that, when expressed independently, are able to restore ion channel functionality (14). The strategy to reassemble functional receptor proteins from non-functional modules takes advantage of the domain architecture of ion channels. Domain swapping experiments between different ion channel subunits have been shown to preserve receptor function in various receptor families, such as the glycine receptor with the prokaryotic GLIC or different glutamate receptors (24, 25). For GlyR, nonsense and frameshift mutations have been described in patients suffering from hyperekplexia, a rare neuromotor disorder (20, 26). A similar hyperekplexia-like phenotype was observed in the GlyR mouse mutant *oscillator*, resulting from lack of GlyR expression due to introduction of a premature stop codon at amino acid position

355 (21). Loss of receptor proteins has also been found in other channelopathies, such as GEFS+ (generalized epilepsy with febrile seizures plus) associated with truncated $GABA_A$ receptor variants (27).

Functionality of the truncated non-functional GlyRα1 variant from the mouse mutant *oscillator* was restored *in vitro* in HEK293 cells and primary spinal cord neurons by coexpression with an independent complementation domain (28). The restoration of GlyR functionality in the two-domain approach exhibited 50% of wild type activity. Here, large truncations of the TM3-4 loop of the complementation domain resulted in loss of functionality. We set out to identify crucial subdomains of the TM3-4 loop that enable an assembly from independent domains. Sequence alignments of all GlyR subunits showed that the TM3-4 loop is of highest variability among GlyR members. The constant region C1 harbors a multifunctional basic motif, which has previously been shown to be important for cell surface expression, subunit-specific sorting, and binding to G$\beta\gamma$ proteins (10, 15, 16). This motif, RRKRRH, is present at the C-terminal end of truncated GlyRα1 (C1 domain) and enhances the efficiency of ion channel rescue by an increase in plasma membrane integration not only of α1-trc but also of the complementation construct (14). In this study, we used the truncated α1 with the RRKRRH motif present to ensure cell surface expression. Stepwise deletion of the complementation construct up to almost C3 (iDΔ62-TM4 to iDΔ67-TM4) resulted in a slight decrease in overall membrane expression. This decrease was coexistent with lower membrane expression of α1-trc, again corroborating the concomitant transport of receptor domains from the ER toward the plasma membrane (14, 28). Interestingly, the amount of cell surface protein observed for iDΔ67-TM4 was indistinguishable from the other complementation constructs. Although protein biogenesis seemed unaffected, the rescue efficiency as a determinant for ion channel functionality in a two-domain receptor configuration dropped severely between truncations of 49–62 amino acids of the N-terminal part of the TM3-4 loop (between V2 and C3). Our data clearly show that the variable region V2 and the conserved region C2 were not responsible for this effect. The V2 region consists of two motifs, one polyasparagine motif (^{394}NNNN^{397}) and a polyproline motif (^{401}PPPAP^{405}). The importance of ^{394}NNNN^{397} in GlyRs is so far unknown; however, protein aggregation studies on proteins such as huntingtin in yeast cells have demonstrated that polyasparagine stretches tend to aggregate and form polar zippers (29, 30). Lack of PPPAP as in the construct iDΔ49-TM4 decreased GlyR rescue efficiency to 58%, suggesting that this motif may be of some importance for the correct GlyR configuration, yet the lower efficiency of ion channel rescue could also be a consequence of continuous protein truncation and therefore loss of steric contact surfaces. Constructs iDΔ55-TM4, iDΔ62-TM4, and iDΔ67-TM4 comprise positively charged N termini. Coexpression of truncated GlyRα1 with these variants lacking parts of the conserved region C3 resulted in almost non-functional ion channels. This observation might be explained by the positively charged N termini of both constructs. The α1-trc domain harbors the RRKRRH motif at its C terminus corresponding to the C1 region. Previous data have demonstrated that a coexpression of truncated α1 together with a complementation domain, which harbors positively charged residues at its N-terminal portion, abolished ion channel function. Thus, GlyR complex stability necessary for rescue of ion channel function was impaired when both intracellular ends were positively charged (14). With iDΔ55-TM4, iDΔ62-TM4, and iDΔ67-TM4, a similar overall configuration was created.

Orientation of proteins with only one TM depends on the strength of topogenic signals formed by positively charged residues next to transmembrane helices (31). Although positively charged residues are an important topological determinant, a local effect of distance from a charged residue to the next TM is still not completely understood (23). Despite the disability of functional reconstitution with iDΔ62-TM4, the number of positively charged amino acids at the intracellular N-terminal part was sufficient to allow a correct orientation of TM4 according to GlyR topology.

We hypothesized that a protein-protein interaction within subdomains of the α1 TM3-4 loop might be required for ion channel opening. Protein-protein interaction of the TM3-4 loop of GlyRβ with the synaptic scaffold protein gephyrin has been shown to be critical for the equilibrium between synaptic and extrasynaptic GlyRs (32). Studies on the movement and interaction of numerous residues in the large extracellular domain of various Cys-loop receptors have provided detailed knowledge of the ligand-binding pocket for several members of this superfamily (7, 33). If GlyRs are expressed in a two-domain configuration, protein interactions are still detectable regardless of the length of the deletion at the N terminus of the complementation constructs. Thus, a lack of an intermolecular protein-protein interaction can be excluded as the reason for the decrease in ion channel rescue efficiency. TM4 most probably serves as a structural component for oligomerization of the receptor complex (34). However, all complementation constructs still contain TM4, and therefore oligomerization is enabled. Although both GlyR domains are present at the plasma membrane, the lacking subdomain of the TM3-4 loop(357–418) seems to comprise a critical determinant required to allow conformational changes and thereby the transduction of ligand binding into channel opening.

As proposed by Bocquet *et al.* (35), a movement following binding of ligand is passed through the whole protein. Rearrangements of several loop structures in the N-terminal part after ligand binding as well as drug-bound or drug-free conformations of other Cys-loop receptors have been investigated with a primary focus on the N-terminal and the transmembrane domains (36). Due to the lack of crystal structures of the large intracellular domain for any kind of Cys-loop receptors, the structural clues for the TM3-4 loop function are scarce. Recently, Breitinger *et al.* (37) reported a correlation of differences in channel gating with the distribution of charged residues in a splice region of the GlyRα3 subunit. Here, we identified the subdomain Leu^{357}–Gln^{418} (V1-C2-V2 half of C3) in the TM3-4 loop of GlyRα1, which enables both the α1-trc and the complementation domain to procure in a distinct configuration, accompanied by a passing movement from TM3 to TM4 and thereby ion channel opening. Nevertheless, we could not exclude the possibility that this subdomain of the TM3-4 loop

interacts with another, thus far unidentified, intracellular protein. In turn, such an interaction could enable a recruitment of the TM3-4 loop subdomain together with the unknown partner to the plasma membrane and concomitantly lead to an interaction with the other independent GlyR domains by chance, resulting in some GlyR functionality. The functional three-domain architecture of GlyRs is consistent with the modular architecture of Cys-loop receptors composed of independently folding domains. Our data on GlyR domain complementation further support a model system for novel gene therapeutic strategies concerning restoration of ion channel dysfunction.

Acknowledgments—We thank Dr. Martin Eberhardt for critical reading of the manuscript and helpful comments. Especially acknowledged are Marina Wenzel and Rosa Weber for excellent technical assistance. Dr. Nima Melzer is gratefully acknowledged for providing the initial sequence alignment of various GlyR subunits.

REFERENCES

1. Lynch, J. W. (2009) Native glycine receptor subtypes and their physiological roles. *Neuropharmacology* **56,** 303–309
2. Villmann, C., and Becker, C. M. (2009) Glycine receptors. in *Ion channels from structure to function* (Kew, J., and Davies, C., eds) pp. 251–263, Oxford University Press, Oxford
3. Dutertre, S., Drwal, M., Laube, B., and Betz, H. (2012) Probing the pharmacological properties of distinct subunit interfaces within heteromeric glycine receptors reveals a functional $\beta\beta$ agonist-binding site. *J. Neurochem.* **122,** 38–47
4. Grudzinska, J., Schemm, R., Haeger, S., Nicke, A., Schmalzing, G., Betz, H., and Laube, B. (2005) The β subunit determines the ligand binding properties of synaptic glycine receptors. *Neuron* **45,** 727–739
5. Vogel, N., Kluck, C. J., Melzer, N., Schwarzinger, S., Breitinger, U., Seeber, S., and Becker, C. M. (2009) Mapping of disulfide bonds within the amino-terminal extracellular domain of the inhibitory glycine receptor. *J. Biol. Chem.* **284,** 36128–36136
6. Hilf, R. J., and Dutzler, R. (2008) X-ray structure of a prokaryotic pentameric ligand-gated ion channel. *Nature* **452,** 375–379
7. Nury, H., Van Renterghem, C., Weng, Y., Tran, A., Baaden, M., Dufresne, V., Changeux, J. P., Sonner, J. M., Delarue, M., and Corringer, P. J. (2011) X-ray structures of general anesthetics bound to a pentameric ligand-gated ion channel. *Nature* **469,** 428–431
8. Kim, E. Y., Schrader, N., Smolinsky, B., Bedet, C., Vannier, C., Schwarz, G., and Schindelin, H. (2006) *EMBO J.* **25,** 1385–1395
9. Saiyed, T., Paarmann, I., Schmitt, B., Haeger, S., Sola, M., Schmalzing, G., Weissenhorn, W., and Betz, H. (2007) Molecular basis of gephyrin clustering at inhibitory synapses. Role of G- and E-domain interactions. *J. Biol. Chem.* **282,** 5625–5632
10. Yevenes, G. E., Moraga-Cid, G., Guzmán, L., Haeger, S., Oliveira, L., Olate, J., Schmalzing, G., and Aguayo, L. G. (2006) Molecular determinants for G protein $\beta\gamma$ modulation of ionotropic glycine receptors. *J. Biol. Chem.* **281,** 39300–39307
11. Moraga-Cid, G., Yevenes, G. E., Schmalzing, G., Peoples, R. W., and Aguayo, L. G. (2011) A Single phenylalanine residue in the main intracellular loop of α1 γ-aminobutyric acid type A and glycine receptors influences their sensitivity to propofol. *Anesthesiology* **115,** 464–473
12. Yevenes, G. E., Moraga-Cid, G., Peoples, R. W., Schmalzing, G., and Aguayo, L. G. (2008) A selective G $\beta\gamma$-linked intracellular mechanism for modulation of a ligand-gated ion channel by ethanol. *Proc. Natl. Acad. Sci. U.S.A.* **105,** 20523–20528
13. Jansen, M., Bali, M., and Akabas, M. H. (2008) Modular design of Cys-loop ligand-gated ion channels. Functional 5-HT3 and GABA rho1 receptors lacking the large cytoplasmic M3M4 loop. *J. Gen. Physiol.* **131,** 137–146
14. Villmann, C., Oertel, J., Ma-Högemeier, Z. L., Hollmann, M., Sprengel, R., Becker, K., Breitinger, H. G., and Becker, C. M. (2009) Functional complementation of Glra1(spd-ot), a glycine receptor subunit mutant, by independently expressed C-terminal domains. *J. Neurosci.* **29,** 2440–2452
15. Melzer, N., Villmann, C., Becker, K., Harvey, K., Harvey, R. J., Vogel, N., Kluck, C. J., Kneussel, M., and Becker, C. M. (2010) Multifunctional basic motif in the glycine receptor intracellular domain induces subunit-specific sorting. *J. Biol. Chem.* **285,** 3730–3739
16. Sadtler, S., Laube, B., Lashub, A., Nicke, A., Betz, H., and Schmalzing, G. (2003) A basic cluster determines topology of the cytoplasmic M3-M4 loop of the glycine receptor α1 subunit. *J. Biol. Chem.* **278,** 16782–16790
17. Chen, C., and Okayama, H. (1987) High efficiency transformation of mammalian cells by plasmid DNA. *Mol. Cell Biol.* **7,** 2745–2752
18. UniProt Consortium (2009) The Universal Protein Resource (UniProt) 2009. *Nucleic Acids Res.* **37,** D169–D174
19. Notredame, C., Higgins, D. G., and Heringa, J. (2000) T-Coffee. A novel method for fast and accurate multiple sequence alignment. *J. Mol. Biol.* **302,** 205–217
20. Tsai, C. H., Chang, F. C., Su, Y. C., Tsai, F. J., Lu, M. K., Lee, C. C., Kuo, C. C., Yang, Y. W., and Lu, C. S. (2004) Two novel mutations of the glycine receptor gene in a Taiwanese hyperekplexia family. *Neurology* **63,** 893–896
21. Kling, C., Koch, M., Saul, B., and Becker, C. M. (1997) The frameshift mutation oscillator (Glra1(spd-ot)) produces a complete loss of glycine receptor α1-polypeptide in mouse central nervous system. *Neuroscience* **78,** 411–417
22. Hessa, T., Kim, H., Bihlmaier, K., Lundin, C., Boekel, J., Andersson, H., Nilsson, I., White, S. H., and von Heijne, G. (2005) Recognition of transmembrane helices by the endoplasmic reticulum translocon. *Nature* **433,** 377–381
23. Seppälä, S., Slusky, J. S., Lloris-Garcerá, P., Rapp, M., and von Heijne, G. (2010) Control of membrane protein topology by a single C-terminal residue. *Science* **328,** 1698–1700
24. Duret, G., Van Renterghem, C., Weng, Y., Prevost, M., Moraga-Cid, G., Huon, C., Sonner, J. M., and Corringer, P. J. (2011) Functional prokaryotic-eukaryotic chimera from the pentameric ligand-gated ion channel family. *Proc. Natl. Acad. Sci. U.S.A.* **108,** 12143–12148
25. Villmann, C., Hoffmann, J., Werner, M., Kott, S., Strutz-Seebohm, N., Nilsson, T., and Hollmann, M. (2008) Different structural requirements for functional ion pore transplantation suggest different gating mechanisms of NMDA and kainate receptors. *J. Neurochem.* **107,** 453–465
26. Becker, K., Hohoff, C., Schmitt, B., Christen, H. J., Neubauer, B. A., Sandrieser, T., and Becker, C. M. (2006) *Hum. Mutat.* **27,** 1061–1062
27. Kang, J. Q., Shen, W., and Macdonald, R. L. (2009) The GABRG2 mutation, Q351X, associated with generalized epilepsy with febrile seizures plus, has both loss of function and dominant-negative suppression. *J. Neurosci.* **29,** 2845–2856
28. Valkova, C., Albrizio, M., Röder, I. V., Schwake, M., Betto, R., Rudolf, R., and Kaether, C. (2011) Sorting receptor Rer1 controls surface expression of muscle acetylcholine receptors by ER retention of unassembled alpha-subunits. *Proc. Natl. Acad. Sci. U.S.A.* **108,** 621–625
29. Peters, T. W., and Huang, M. (2007) Protein aggregation and polyasparagine-mediated cellular toxicity in *Saccharomyces cerevisiae*. *Prion* **1,** 144–153
30. Perutz, M. F., Pope, B. J., Owen, D., Wanker, E. E., and Scherzinger, E. (2002) Aggregation of proteins with expanded glutamine and alanine repeats of the glutamine-rich and asparagine-rich domains of Sup35 and of the amyloid β-peptide of amyloid plaques. *Proc. Natl. Acad. Sci. U.S.A.* **99,** 5596–5600
31. Hessa, T., White, S. H., and von Heijne, G. (2005) Membrane insertion of a potassium-channel voltage sensor. *Science* **307,** 1427
32. Specht, C. G., Grünewald, N., Pascual, O., Rostgaard, N., Schwarz, G., and Triller, A. (2011) Regulation of glycine receptor diffusion properties and gephyrin interactions by protein kinase C. *EMBO J.* **30,** 3842–3853
33. Hibbs, R. E., and Gouaux, E. (2011) Principles of activation and permeation in an anion-selective Cys-loop receptor. *Nature* **474,** 54–60
34. Haeger, S., Kuzmin, D., Detro-Dassen, S., Lang, N., Kilb, M., Tsetlin, V., Betz, H., Laube, B., and Schmalzing, G. (2010) An intramembrane aro-

matic network determines pentameric assembly of Cys-loop receptors. *Nat. Struct. Mol. Biol.* **17,** 90–98

35. Bocquet, N., Nury, H., Baaden, M., Le Poupon, C., Changeux, J. P., Delarue, M., and Corringer, P. J. (2009) X-ray structure of a pentameric ligand-gated ion channel in an apparently open conformation. *Nature* **457,** 111–114
36. Miller, P. S., and Smart, T. G. (2010) Binding, activation, and modulation of Cys-loop receptors. *Trends Pharmacol. Sci.* **31,** 161–174
37. Breitinger, H. G., Villmann, C., Melzer, N., Rennert, J., Breitinger, U., Schwarzinger, S., and Becker, C. M. (2009) Novel regulatory site within the TM3-4 loop of human recombinant α3 glycine receptors determines channel gating and domain structure. *J. Biol. Chem.* **284,** 28624–28633